4-1-1989

Ionization from Soft Electron Precipitation in the Auroral F Region

J. Labelle

R. J. Sica

C. Kletzing

G. D. Earle

M. C. Kelley

D. Lummerzheim

See next page for additional authors

JOURNAL OF GEOPHYSICAL RESEARCH, VOL. 94, NO. A4, PAGES 3791–3798, APRIL 1, 1989
Labelle, J., R. J. Sica, C. Kletzing, G. D Earle, M. C. Kelley, D. Lummerzheim, R. B. Torbert, K. D. Baker, and G. Berg. 1989. "Ionization from Soft Electron Precipitation in the Auroral *F* Region." *Journal of Geophysical Research* 94 (A4) 3791–98. doi:10.1029/JA094iA04p03791.

Ionization From Soft Electron Precipitation in the Auroral *F* Region

J. LABELLE,[1] R. J. SICA,[1,2] C. KLETZING,[3,4] G. D. EARLE,[5] M. C. KELLEY,[5] D. LUMMERZHEIM,[6] R. B. TORBERT,[7] K. D. BAKER,[1] AND G. BERG[1,8]

Rocket-borne instrumentation, launched into the morning sector auroral zone from Sondre Stromfjord, Greenland, detects electron density enhancements correlated with enhancements in the flux of soft (less than 1 keV) downgoing electrons. These electron density enhancements seem most likely to have been generated by direct production of ionization at *F* region altitudes. Model calculations of the electron impact ionization rate, based on the measured electron spectrum, lend support to this hypothesis.

INTRODUCTION

The highly structured nature of the high-latitude *F* region at a variety of scale sizes from centimeters to hundreds of kilometers has been confirmed by a large number of measurements, including ionosonde measurements [e.g., *Sato and Rourke,* 1964], incoherent scatter radar measurements [e.g., *Banks et al.,* 1974; *Vickrey et al.,* 1980; *Kelley et al.,* 1982; *Robinson et al.,* 1985; *Tsunoda et al.,* 1985], rocket measurements [e.g., *Kelley et al.,* 1982], satellite measurements [e.g., *Dyson et al.,* 1974; *Clark and Raitt,* 1976; *Phelps and Sagalyn,* 1976; *Rodriguez and Szuszczewicz,* 1984; *Basu et al.,* 1988], scintillation measurements [e.g., *Aarons et al.,* 1969; *Rino and Mathews,* 1979], as well as combinations of these and other measurements [e.g., *Kelley et al.,* 1980; *Weber et al.,* 1985; *Basinska et al.,* 1987]. In general, the density structures at the small-scale end of this range probably result from plasma instabilities, while the generation of the large-scale structures is most likely dominated by production/loss processes and convection (see, for example, discussion in the work by *Kelley et al.* [1982]). For the in-between scale sizes (hundreds of meters to ten kilometers), both instabilities as well as ion production and convection probably play an important role.

In this paper we will be concerned primarily with the large-scale regime, i.e., structures greater than 10 km. The salient features in this regime are the often reported plasma "blobs." These were first reported by *Banks et al.* [1974] and have been studied by a number of observers since then (R. T. Tsunoda, High-latitude *F* region irregularities: A review and synthesis, submitted to *Rev. Geophys. Space Phys.,* 1988). These features have been observed throughout the high latitude and polar cap region. As *Kelley et al.* [1982] point out, the lifetime for such large structures, determined by the diffusion time, is very long, implying that once formed they may be convected great distances across the polar cap by the electric field. Indeed, *Weber et al.* [1984] present strong experimental evidence for the convection of the blobs across the polar cap. *Sojka and Schunk* [1986] have modeled the evolution of density structure in the high-latitude ionosphere and also conclude that these structures can convect long distances across the polar cap, although they find that the evolution of the structures is quite complex, with a great deal of structuring arising due to variations in the ionospheric convection electric field. The generation of the blobs is still a subject of some controversy. *Kelley et al.* and others (see review by *Fejer and Kelley* [1980]) have shown evidence for the importance of soft electron precipitation in generating large-scale structures, with the source region perhaps concentrated in an annular ring of diffuse precipitation at the poleward edge of the oval. On the other hand, *de la Beaujardiére et al.* [1985] show evidence based on the universal time dependence of the blobs which suggests that the dominant generation mechanism may be solar EUV photoionization at the dayside, an idea first put forth by *Sato and Rourke* [1964].

In this paper we shall show further evidence that soft electron precipitation can be a source of significant density enhancements in the high-latitude *F* region. Although a determination of the relative importance of the generation mechanisms for the large-scale structure is far beyond the scope of this study, our data do indicate that the soft electron ionization merits further attention, particularly at scales from 10 to 100 km.

ROCKET MEASUREMENTS

NASA rocket 29.023 was launched from Sondre Stromfjord, Greenland (67° north, 51° west geographic), on January 23, 1985, at 0923 UT, corresponding to approximately 0800 magnetic local time. The rocket was launched in a magnetic southeasterly direction into the dayside auroral oval, which was characterized by sunward convection as determined from simultaneous incoherent scatter measurements by the Sondre Stromfjord radar. The payload reached an apogee of 500 km, and during the flight it traversed several auroral arcs, which were detectable visually, from all-sky camera data, and from their signatures in the rocket particle, density, and electric field data.

The particle detectors, provided by the University of California at San Diego, included measurements of the electron distribution function with 87-ms time resolution, obtained from a hemispherical electrostatic analyzer which measured 19 pitch angle channels simultaneously. This detector was swept over energies from 17 eV to 17 keV. Due to coning motion of the

[1]Center for Atmospheric and Space Sciences, Utah State University, Logan, Utah.
[2]Also at Department of Physics, University of Western Ontario, London, Ontario.
[3]Department of Physics, University of California at San Diego, La Jolla, California.
[4]Also at Department of Physics, University of Alabama at Huntsville, Huntsville, Alabama.
[5]School of Electrical Engineering, Cornell University, Ithaca, New York.
[6]Geophysical Institute, University of Alaska, Fairbanks, Alaska.
[7]Department of Physics, University of Alabama, Huntsville, Alabama.
[8]Now at School of Electrical Engineering, Cornell University, Ithaca, New York.

Paper number 88JA04086.
0148-0227/89/88JA-04086$02.00

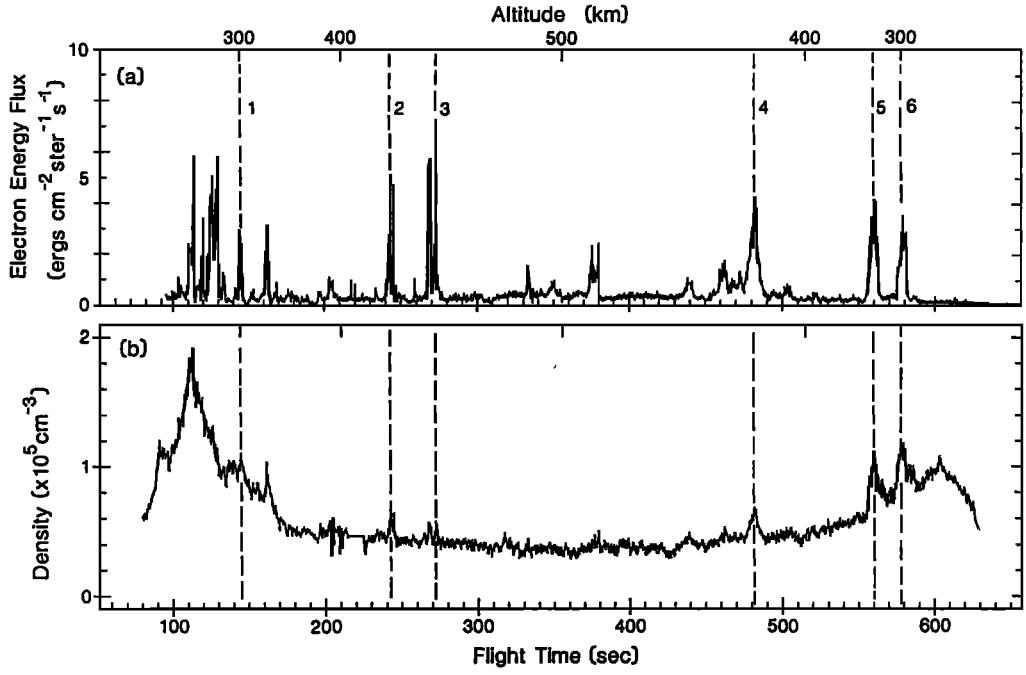

Fig. 1. (*a*) Downward angular electron energy flux and (*b*) absolute electron density measured during the flight of NASA rocket 29.023 (January 23, 1985). The absolute density was obtained by normalizing the Langmuir probe collected current to a plasma frequency probe. The angular electron energy flux is for the upward looking detector and is integrated over the energy range 17–2000 eV. Vertical dashed lines indicate some of the enhancements in the density which are coincident with enhancements in the downward going electron flux.

rocket, the pitch angle coverage was sometimes uneven. The measurements of absolute energetic electron number and energy fluxes used in this paper are accurate to within a factor of 2–3, and the relative measurement of electron fluxes is accurate to 20–40%. (For details of the instrument, see *Kletzing* [1989].) The absolute plasma density was measured by means of a Plasma Frequency Probe (PFP) provided by Utah State University. This instrument measures the plasma density with better than millisecond time resolution by detecting the upper hybrid resonance of the plasma [*Baker et al.,* 1969]. In addition, the relative ion density was obtained from a negatively biased Langmuir probe provided by Cornell University. Other instruments on board measured the electric field and energetic ions, but these will not be discussed further here.

Figure 1*b* shows an overview of the plasma density for the entire flight [*Earle,* 1988]. These data are plotted as a function of flight time, with the corresponding altitudes indicated at the top of the figure. Unfortunately, the PFP was ineffective throughout much of the topside *F* region (times from 160 to 570 s) due to the low density there. Hence the density shown in Figure 1*b* has been obtained from the Langmuir probe collected current, normalized to the PFP during the portions of the flight when the PFP made absolute density measurements. This technique of normalizing the collected current to the absolute density can be tricky in the *E* region where the density and temperature (and hence the Debye length) change by an order of magnitude or more [*Baker et al.,* 1985], but in the upper *F* region (above 300 km) where the density changes much more gradually, normalizing the Langmuir probe data provides a fairly accurate measurement of the absolute density (e.g., Figure 3*a* of *LaBelle et al.* [1986]). The density measurement is therefore probably accurate to within 10–30%.

Figure 1*b* shows that on both the upleg and the downleg of the rocket flight, the density maximizes in the *F* region near 200 km altitude and then, except for the short-duration bursts which are discussed in detail below, monotonically decreases up to 500 km, the highest altitude reached by the payload. The downleg *F* region is considerably less dense than the upleg *F* region. The reason for this is not clear, but the observation is in agreement with simultaneous data from the Sondre Stromfjord radar and a companion rocket launch; most likely, the enhanced density is related to precipitating electrons, which were abundant during upleg *F* region traversal. In any case, aside from the *F* region itself, the most noteworthy features in the density data are a number of spikes, six of which are indicated by vertical lines in the figure. These represent enhancements in the electron density of $1 - 5 \times 10^4$ cm^{-3}. Their time duration is 10–20 s, corresponding to 10–20 km if these structures are stationary and aligned with the roughly vertical magnetic field. (The rocket horizontal velocity was about 1 km/s.)

Figure 1*a* shows the downgoing electron angular energy flux, integrated over electron energies from 0.01 to 2.0 keV; i.e., the relatively soft electrons which comprised the bulk of the observed precipitation. This figure shows that all of the electron density spikes correspond to enhanced fluxes of soft electrons. These enhancements involve peak angular energy fluxes of 3–7 ergs cm^{-2} st^{-1} s^{-1} in the downward direction and time durations of 10–20 s, identical to the durations of the corresponding density enhancements. When the electron spectra are examined, it is seen that the mean energy during these enhancements is 200–500 eV, and the events labeled 4–6 are characterized by the classic inverted-V structure in the particle spectrograms. These enhancements in the electron flux almost certainly correspond to traversals of weak auroral arcs by the payload, although a

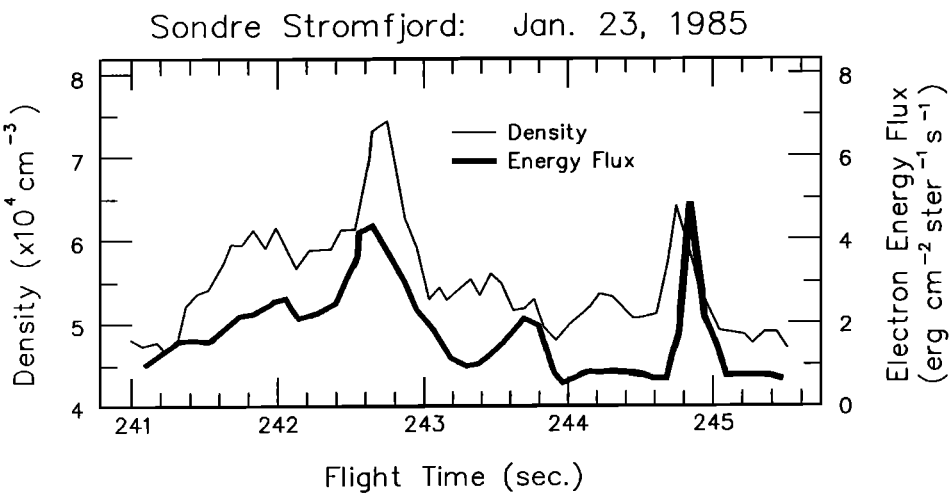

Fig. 2. An expanded view of the electron density and downward electron angular energy flux for the event labeled 2 in Figure 1. This figure shows that the two quantities are indeed highly correlated with essentially zero time lag.

direct correlation with optical data is not possible. Besides the six electron flux enhancements which are indicated by vertical lines in the figure, a number of others occur, and in every case some sort of density enhancement coincides, although not in every case is the coincidence as unambiguous as in the six cases indicated. The *F* region peak observed near 200 km during the upleg also shows evidence for enhanced downward electron flux, indicating that its unusual form and elevated density (compared with the downleg *F* layer) may be controlled by the soft precipitation as well.

Figure 2 is an expanded plot of the plasma density and the downward angular electron energy flux corresponding to the event labeled 2 in Figure 1. This plot shows that even on time scales of 1 s the correlation between these two measurements is very high and that there is essentially no time lag between the peak in density and that in the electron flux. In some cases, as near $t = 245$ in Figure 2, the downgoing electron energy flux appears somewhat more sharply structured than the electron density, but at other times this effect is not as apparent.

As discussed above, there are a number of possible sources for large-scale density structure in the auroral *F* region. These include the convection of structures formed by photo-ionization on the dayside, the effect of irregular electric fields on a background density gradient, vertical diffusion of enhanced plasma generated by ionization at lower altitudes, and direct production of ionization locally by soft electron precipitation. At these large scales, other sources, such as plasma instabilities, are believed to be of lesser importance [*Kelley et al.*, 1982]. For the structures shown in Figure 1, the mechanism involving photo-ionization seems unlikely due to the "instantaneous" coincidence between the density and the local precipitating electrons. The advection of the background gradient to form structures cannot be completely ruled out, since auroral arcs are associated with electric fields; however, this mechanism seems unlikely, since only density enhancements are observed, whereas the advection effect should also produce density depletions. Also, there is no evidence in simultaneous radar data for the large horizontal density gradients which would be required by this explanation. Finally, since the diffusion time along the field line is very long compared with the time for which the arcs are stationary (the order of minutes), it seems unlikely that the dominant mechanism involves production of ionization at lower altitudes followed by upward diffusion, a process which would not be capable of producing such sharp coincident features in the density and the precipitating electrons. In conclusion, it appears most likely that the excellent correlation between the density structure and the measured precipitating electrons arises because of direct local production of the density enhancements by impact ionization from the soft electrons. The fact that the electron flux sometimes exhibits sharper structure than the density is consistent with this hypothesis, since there are several possible processes, such as diffusion, transport, or motion of the arc itself, which might act to broaden the density structure relative to the observed instantaneous structure of the arc.

Kelley et al. [1982] put forth the same hypothesis to explain rocket data obtained under similar conditions. Their result was subject to uncertainty, however, since the collected current from a constant-voltage-biased Langmuir probe was the only means of monitoring electron density. The energetic electrons can enhance the collected current independent of the density by production of ions and secondaries when they strike the probe, and although this effect should be relatively small depending on the ambient density, some uncertainty persisted concerning the contamination of the Langmuir probe measurement by the electron precipitation. In the present case, however, the direct detection of three of the six events using the plasma frequency probe *in addition to* the Langmuir probe eliminates these uncertainties. In the three cases where overlapping Langmuir probe and plasma frequency probe data exist, there are some small differences in the profile of the events, the order of 10–30%, with the collected current always giving too high a density. This indicates that the Langmuir probe data may indeed be affected by contamination effects, but these effects are not important to the results of this study.

To test the hypothesis that the soft electron precipitation directly produces the observed density structures through electron impact ionization, it is desirable to calculate whether the observed enhanced electron spectrum can produce adequate local enhancements in the electron density in the *F* region. This problem is similar to the *E* region study of *Vondrak and Robinson* [1985], in which satellite measured electron spectra

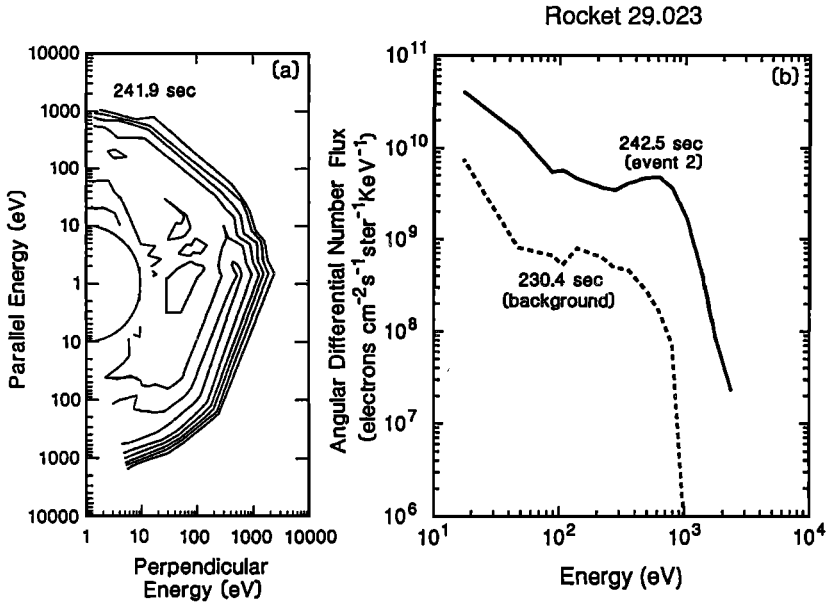

Fig. 3. The electron distribution corresponding to the peak in electron energy flux labeled 2 in Figure 1 (437 km). The left-hand panel is a contour plot of the angular differential energy flux as a function of perpendicular and parallel energy, showing that the peak in the energy flux at a few hundred eV is restricted to the downgoing hemisphere but is more or less isotropic in that hemisphere. The unusual straightness of the contours at certain pitch angles is due to bunching of the pitch angle channels arising from the rocket's coning motion. The right-hand panel shows the angular differential number flux as a function of energy for the downgoing electrons and represents the spectrum used to model the ionization rate. The dashed curve indicates the background level determined from the electron spectrum approximately 10 s before event 2.

for the energy range 0.2–25 keV were used to predict the *E* region density structure measured with the Chatanika incoherent scatter radar. Similarly, a number of previous papers have applied measured electron spectra in combination with a model to predict optical emissions as a function of altitude [e.g., *Arnoldy and Lewis*, 1977; *Kasting and Hays*, 1977; *Rees et al.*, 1977], and a number of other research efforts have worked the problem backwards, obtaining primary electron spectra from radar measurements of the density in the *E* region [e.g., *Vondrak and Sears*, 1978; *Sears and Vondrak*, 1981; *Vallance-Jones et al.*, 1987]. Relatively few of these studies deal with *F* region altitudes and very soft electrons, however. Although even very soft (≈100 eV) electrons create the bulk of their ionization in the lower *F* region or upper *E* region, the ionization rate at 300–500 km is not zero and is probably adequate to explain the observed density enhancements. To investigate this, we turn now to a model calculation of the ionization rate.

Modeling Studies

An electron transport model developed at the University of Alaska for predicting auroral optical emissions from precipitating electron fluxes [*Lummerzheim*, 1987*a*; *Lummerzheim et al.*, 1989] has been used to calculate the ionization rates in the *F* region from the measured incident electron spectra. This model solves a time-independent, one-dimensional electron transport equation, which is derived from the Boltzmann equation. The transport equation neglects three- and multiple-body collisions, implying that the Boltzmann collision integral may be expressed as the difference between the sources and losses in a given phase space volume. These sources and losses are given by differential cross sections, which describe elastic and inelastic interaction between streaming electrons and ambient neutrals. The model employs the energy degradation method of *Swartz* [1985] and the discrete ordinate method of *Stamnes et al.* [1988] for the transport along the geomagnetic field, and it includes elastic, excitation, dissociation, and ionization collisions with the neutral constituents of the upper atmosphere as well as energy loss to the ambient electron gas. Given the observed electron spectrum at the rocket altitude, the electron intensity is computed as a function of energy, pitch angle, and altitude for the region beneath the incident electron precipitation. The ionization rates are then calculated from the incident electron spectrum, the energy degraded secondary electrons, and the backscattered electron spectrum.

For this study, the mass spectrometer/incoherent scatter (MSIS) MSIS 86 empirical neutral atmosphere [*Hedin*, 1987] was used with the relevant geophysical parameters for the exact locations and times of the rocket measurements. Lacking independent information on the composition of the neutral atmosphere from simultaneous optical observations or *in situ* measurements, the MSIS 86 model outputs were used without modification. Since the dominant species in the *F* region is atomic oxygen, the uncertainties of our results are governed by the uncertainty of the O density, which can be as large as 50% [*Roble et al.*, 1984].

Typical of the six electron spectra modeled is event 2 (0927 UT). Figure 3*a* shows the pitch angle dependence of the angular differential energy flux of the electrons for this event, which is essentially isotropic in the downward hemisphere. The downward angular electron number flux as a function of energy near the peak of this event is shown in Figure 3*b*, along with the background level of the angular differential number flux spectrum as measured approximately 10 s before event 2. Note that the spectrum from the event is soft, with the high-energy peak at about 650 eV and a mean energy of 240 eV. (The mean energy is defined to be the ratio of the downward energy flux to the

number flux.) This spectrum was used as an input to the electron transport code to calculate ionization rates for producing N_2^+, O_2^+, and O^+. Though the code is capable of multistream calculations (for modeling complex pitch angle distributions), for this study a two-stream calculation was made. The impact of not resolving the hemispherical pitch angle distribution for these nearly isotropic electron spectra is negligible compared with the uncertainties in the neutral density profiles [*Lummerzheim*, 1987*b*].

The spectrum in Figure 3*b* is only shown up to 2500 eV, since the detector was at its noise level for all larger energies. The high-energy peaks of all spectra modeled from this flight were below 1000 eV, and the number flux at 2500 eV was in every case about 3 orders of magnitude lower than at the high-energy peak. To be certain that the number density of higher energy electrons below the threshold of the instrument did not affect the ionization rates, the calculation was repeated with a high-energy tail extrapolated from the measurements. Because of the low energy flux at these energies, this extension had no appreciable effect on the ionization rates.

Figure 4 shows altitude profiles of the calculated ionization rates for N_2^+, O_2^+, and O^+ corresponding to the event shown in Figures 2 and 3 and labeled 2 in Figure 1. For this very soft spectrum, the peak of the ionization and energy deposition rates is at about 150 km, where N_2^+ ion production dominates. Above about 240 km O^+ ion production becomes dominant. Between 300 and 400 km the total ion production from electron impact on neutrals varies from about 100 to 1000 cm^{-3} s^{-1}. Note that the calculations do not include photoionization or chemical ion sources. The solar depression angle varied from about 17° to 14° during the flight, so photoionization should be negligible at the rocket's altitude in aurorae. To check this assumption the photoionization model of *Rasmussen et al.* [1988] was run for the appropriate geophysical conditions of the rocket flight. Total photoionization rates varied between 0.04 and 0.65 cm^{-3} s^{-1}, and hence only auroral ionization need be considered.

To verify that the ionization rate is indeed enhanced at the rocket altitude during the events being modeled, the ion production was calculated for the "background" spectrum obtained just before the passage through the density structure and shown

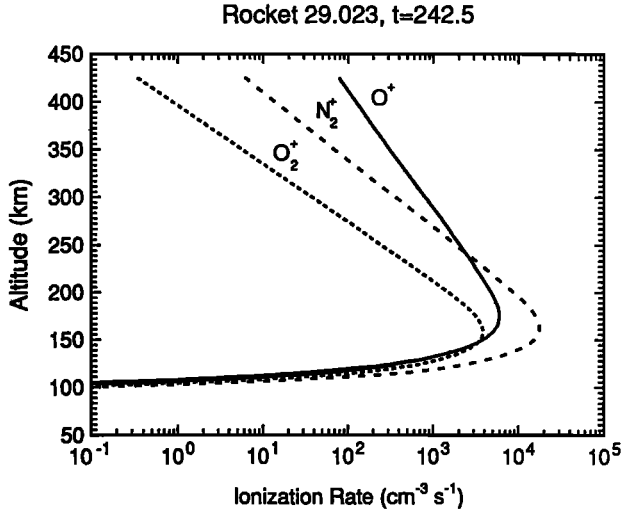

Fig. 4. The ionization rate as a function of altitude for N_2^+, O_2^+, and O^+ calculated assuming an input spectrum given by Figure 3 at 437 km.

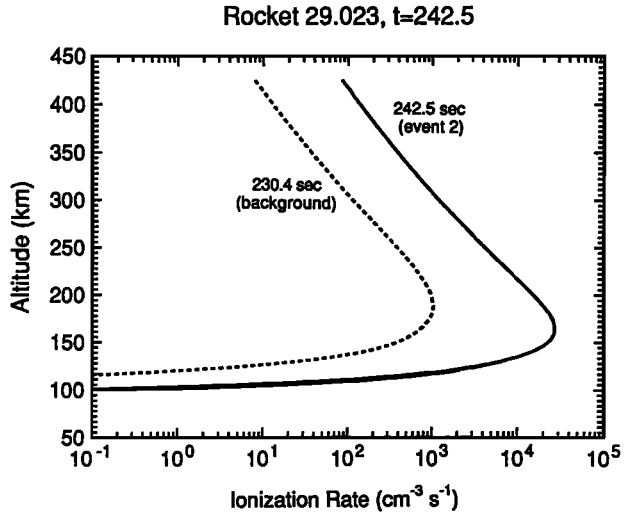

Fig. 5. The total ionization rate as a function of altitude calculated from the electron spectrum measured during event 2 (solid curve) and from a background spectrum measured about 10 s before the event (dashed curve).

as a dashed curve in Figure 3*b*. The angular energy flux in this spectrum is 0.2 ergs cm^{-2} s^{-1} st^{-1}, more than an order of magnitude less than during event 2. Using the background spectrum as an input to the auroral transport model, a total ionization rate is obtained which is shown by the dashed curve in Figure 5. The solid curve in Figure 5 is the total ionization rate corresponding to event 2, obtained by simply adding the three curves shown in Figure 4. Below 250 km, the background ionization rate differs significantly from that corresponding to the density structure, with the peak ion production near 150 km a factor of about 25 higher in the structure. At the rocket altitude, the differences are smaller, but the total ionization rate is still more than an order of magnitude smaller in the background case than in the event itself (8.1 cm^{-3} s^{-1} for the background versus 86 cm^{-3} s^{-1} for event 2).

The ionization rates at rocket altitude for the six density structure events are given in Table 1. In Table 1, all the columns represent either data or information pertaining to the six events except for the ionization rate, which is calculated using the electron transport model, and the required ionization time (δt), which is obtained from the calculated ionization rate and the absolute density enhancement. In three of the six cases, more accurate plasma frequency probe measurements are available and are used instead of the normalized Langmuir probe current to estimate the absolute density enhancements, although in all cases the differences are no more than 30%. The spectral shapes of all six events were similar, with mean energy varying from 240 to 440 eV. Events 2, 4, 5, and 6 correspond to nearly equal downward electron energy flux; event 1 has a somewhat lower energy flux, while event 3 has somewhat higher energy flux. The ionization rates naturally tend to be larger at the lower altitudes where the larger neutral density stops more of the incident energy.

For comparison, we have also calculated the ionization rate for one of the lower-altitude events (event 6 in Table 1 and Figure 1, corresponding to 299 km) with the early model result of *Rees* [1963] to see if the cruder model gives a reasonable approximation of the ionization rate. Rees gives a formula for computing the ionization rate as a function of electron density

TABLE 1. Data from the Six Events Denoted by Vertical Lines in Figure 1, Along With the Calculated Ionization Rate and Required Ionization Time for These Events

Event Number	Time			Altitude, km	Mean Spectral Energy, eV	Angular Energy Flux, erg cm^{-2} s^{-1} st^{-1}	Ionization Rate, cm^{-3} s^{-1}	ΔN_e, $\times 10^4$ cm^{-3}	$\Delta N_e/N_e$, %	Δt, s
	Flight, s	UT	MLT							
1	143	0925	0732	297	362	2.6	1211	2.20*	28*	18*
2	242	0927	0748	439	240	4.4	86	3.02	70	350
3	272	0928	0753	464	280	7.6	138	1.44	35	104
4	483	0931	0825	437	366	4.0	82	2.45	56	300
5	560	0932	0838	332	440	4.1	627	3.00*	43*	48*
6	578	0933	0840	299	360	3.6	1530	3.05*	34*	20*

*For these events, the plasma frequency probe was used to determine ΔN_e rather than the normalized Langmuir probe current.

and altitude, valid for 0.4–300 keV electrons. The experimental spectra in our case are dominated by electrons at the very low end of this energy range, and there is some reason to question the applicability of the Rees model at these energies, since the model is based on extrapolation of laboratory data obtained by *Grün* [1957] at energies of 5–54 keV. Rees finds that at altitudes near 300 km, for a hemispherically isotropic electron distribution, the ionization rate per incident electron is nearly constant with electron energy over the energy range 0.4–1 keV, which covers the characteristic energies of our measured spectra (see Figure 2 of *Rees* [1963]). Multiplying the experimentally determined downward electron number flux for this energy range from event 6 (2.5×10^9 cm^{-2} s^{-1}) by the constant obtained from Figure 2 of Rees and corrected for the MSIS 86 neutral density at the position and time of the rocket during event 6 (1.3×10^{-7} cm^{-1}), we obtain an ionization rate of 327 cm^{-3} s^{-1}. For comparison, using the *Lummerzheim* [1987*a*] model including only the 0.4–2 keV electrons, we obtain an ionization rate of 560 cm^{-3} s^{-1}. Thus the Rees model underestimates the ionization rate from the 0.4–2 keV electrons by almost a factor of two. Furthermore, the ionization rate from the Lummerzheim model with the truncated (0.4–2 keV) electron spectrum is only about 35% of the value obtained using the full spectrum (Table 1). This is not surprising, since the ionization cross section peaks near 100 eV, and this result highlights the importance of the electrons below 400 eV for producing *F* region ionization.

DISCUSSION

The last three columns of Table 1 show, respectively, the measured absolute density enhancement of each event, the measured relative density enhancement ($\Delta N_e/N_e$), and the time required to generate this density enhancement (assuming the calculated ionization rate). Note that although the ionization rate is higher at lower altitudes, as noted above, the ΔN_e in these six cases does not show an altitude dependence, and therefore the time required for the generation of the density structure varies with altitude from 20 to 30 s at 300 km to around 5 min at 450 km. (The time period for the six cases varies from 20–350 s, with a mean of 150 s.) For comparison, a typical recombination time for $N_e \sim 10^4$ cm^{-3} in the *F* region is about 1.5 hours [e.g., *Wickwar et al.*, 1975], far longer than the ion production times and therefore negligible. Typical diffusion times for a 10-km density structure are also much greater, as noted above: the order of an hour due to ions escaping along the field lines [e.g., *Knudsen*, 1974; *Schunk et al.*, 1976]; and at least 5 hours for perpendicular diffusion, even if the Bohm limit is assumed for the diffusion coefficient [*Kelley et al.*, 1982].

It is not known, however, how long the observed arcs remained stationary, since the rocket provides only a snapshot (10–20 s). All-sky photographic measurements were obtained from Sondre Stromfjord, but the rocket was near the horizon at the times of the precipitation events studied here. Unaided observations by the human eye indicated well-defined elongated arcs imbedded in a diffuse background during the flight. There is evidence from the particle signatures that the events indicated in Figure 1, especially numbers 4–6, are more stable than other more impulsive features observed during the flight [*Kletzing*, 1988]. Events 4–6 also correspond to the broadest density structures, indicating that perhaps these events have been stable for a relatively long time. In summary, there is no hard evidence for the stationarity of the arc features other than the time of the rocket traversal itself (10–20 s). However, in the morning sector the oval tends to be rather stable [*Akasofu*, 1968], and hence 5 minutes does not seem at all unreasonable for a weak morning-side auroral arc.

Even if the arc is stationary, one has to consider the possibility that the newly produced plasma may drift out of the production region. The electric field during the flight was primarily southward, but with a zonal component of 10–20 mV/m [*Earle*, 1988], implying a drift velocity of 200–400 m/s. This might in the worst case cause the ions to drift poleward or equatorward out of the production region on a time scale of 25–100 s, provided that the precipitation region has spatial scale of 10–20 km. If the arc itself drifts at the same rate, this time scale is much longer. This spatial resonance effect has been discussed by *Weber et al.* [1984]. In any case, one may conclude empirically that the drift of the plasma out of the precipitation region on a time scale short compared with 150 s is probably not occurring because that would result in the density structure being significantly broader than the precipitation structure, while the observed density structures are either the same or only slightly broader than the precipitation structures (Figure 2).

CONCLUSIONS

We have observed in the auroral *F* region at heights from 300 to 500 km a number of density enhancements, with $\Delta N_e/N_e$ amplitudes of 30–70% ($\Delta N_e \sim 0.5 - 4.0 \times 10^4$ cm^{-3}) and spatial scales the order of 10–20 km (if they are assumed stationary and field aligned). In each case, the density enhancements are correlated with enhancements in the flux of precipitating (downgoing) electrons with mean energies of a few hundred electron volts. The electron flux enhancements and the coincident density enhancements are so highly correlated that production of these density structures through local ionization seems the most

likely explanation of their origin. To test this hypothesis, an electron transport model has been used to determine the ionization rate based on the measured electron spectrum. The calculation shows that 20–350 s are required to create the observed density enhancements. Although no independent evidence could be obtained for the stationarity of the observed auroral structures, 5 minutes is not an unreasonable value for weak auroral features such as these. Hence the modeling lends some plausibility to the conclusion that these particular large-scale density structures arise from local ionization in the *F* region.

Of course, from such a limited data set we cannot make general conclusions concerning the source of all large scale structure in the high-latitude *F* region. Quite possibly such structure arises in general from several different generation mechanisms. However, our data do show that one of those mechanisms is the structuring in the ion production resulting from soft electron precipitation.

Acknowledgements. The rocket experiment reported in this study was made possible by NASA grants NAG 5-603 to Utah State University, NAG 5-634 to the University of Alabama at Huntsville, and NSG-6020 to Cornell University. The modeling effort was supported by AFOSR contract F49620-86-C-0109 to Utah State University and by NSF contracts ATM-87-01192 and ATM-83-12883 to the University of Alaska. Greg Earle was supported by NASA grant NGT-33-010-802, and Craig Kletzing was supported by NASA grant NGT-50131.

The Editor thanks W. R. Hoegy and P. Tanskanen for their assistance in evaluating this paper.

REFERENCES

Aarons, J., J. P. Mullen, and H. E. Whitney, The scintillation boundary, *J. Geophys. Res., 74*, 884, 1969.

Akasofu, S., *Polar and Magnetosphere Substorms*, D. Reidel, Hingham, Mass., 1968.

Arnoldy, R. L., and P. B. Lewis, Jr., Correlation of ground-based and topside photometric observations with auroral electron spectra measurements at rocket altitudes, *J. Geophys. Res., 82*, 5563, 1977.

Baker, K. D., E. F. Pound, and J. C. Ulwick, Digital plasma frequency probe for fine scale ionospheric measurements, in *Small Rocket Instrumentation Techniques*, edited by K. Maeda, North-Holland, p. 49, Amsterdam, 1969.

Baker, K. D., J. LaBelle, R. F. Pfaff, M. C. Kelley, L. C. Howlett, N. B. Rao, and J. C. Ulwick, Absolute electron density measurements in the equatorial ionosphere, *J. Atmos. Terr. Phys., 47*, 781, 1985.

Banks, P. M., C. R. Chapell, and A. F. Nagy, A new model for the interaction of auroral electrons with the atmosphere: spectral degradation, backscatter, optical emission, and ionization, *J. Geophys. Res., 79*, 1459, 1974.

Basinska, E. M., W. J. Burke, Su. Basu, F. J. Rich, and P. F. Fougere, Low-frequency modulation of plasmas and soft electron precipitation near the dayside cusp, *J. Geophys. Res., 92*, 3304, 1987.

Basu, Su, S. Basu, E. MacKenzie, P. F. Fougere, W. R. Coley, N. C. Maynard, J. D. Winningham, M. Sugiura, W. B. Hanson, and W. R. Hoegy, Simultaneous density and electric field fluctuation spectra associated with velocity shears in the auroral oval, *J. Geophys. Res., 93*, 115, 1988.

de la Beaujardière, O., V. B. Wickwar, G. Caudal, J. M. Holt, J. D. Craven, L. A. Frank, L. H. Brace, D. S. Evans, J. D. Winningham, and R. A. Heelis, Universal time dependence of nighttime *F* region densities at high latitudes, *J. Geophys. Res., 90*, 4319, 1985.

Clark, D. H., and W. J. Raitt, The global morphology of irregularities in the topside ionosphere as measured by the total ion current probe on ESRO-4, *Planet. Space Sci., 24*, 873, 1976.

Dyson, P. L., J. P. McClure, and W. B. Hanson, *In situ* measurements of the spectral characteristics of *F* region ionospheric irregularities, *J. Geophys. Res., 79*, 1497, 1974.

Earle, G. D., Electrostatic plasma waves and turbulence near auroral arcs, Ph.D. thesis, Cornell Univ., Ithaca, N.Y., 1988.

Fejer, B. G., and M. C. Kelley, Ionospheric irregularities, *Rev. Geophys., 18*, 401, 1980.

Grün, A. E., Lumineszenz—photometrische Messungen der Energieabsorption im Strahlungsfeld von Elektronenquellen, Eindimensionaler Fall in Luft, *Z. Naturf., 12a*, 89–95, 1957.

Hedin, A. E., MSIS-86 thermospheric model, *J. Geophys. Res., 92*, 4649, 1987.

Kasting, J. F., and P. B. Hays, A comparison between N_2^+ 4278-Å emission and electron flux in the auroral zone, *J. Geophys. Res., 82*, 3319, 1977.

Kelley, M. C., K. D. Baker, J. C. Ulwick, C. L. Rino, and M. J. Baron, Simultaneous rocket probe, scintillation, and incoherent scatter observations of irregularities in the auroral zone ionosphere, *Radio Sci., 15*, 491, 1980.

Kelley, M. C., J. F. Vickrey, C. W. Carlson, and R. Torbert, On the origin and spatial extent of high-latitude *F* region irregularities, *J. Geophys. Res., 87*, 4469, 1982.

Kletzing, C., Ph.D. thesis, Univ. of Calif. San Diego, 1989.

Knudsen, W. C., Magnetospheric convection and the high-latitude F_2 ionosphere, *J. Geophys. Res., 79*, 1046, 1974.

LaBelle, J., M. C. Kelley, and C. E. Seyler, An analysis of the role of drift waves in equatorial spread *F*, *J. Geophys. Res., 91*, 5513, 1986.

Lummerzheim, D., Electron transport and optical emissions in the aurora, Ph.D. thesis, Univ. of Alaska, Fairbanks, 1987*a*.

Lummerzheim, D., On the influence of non-isotropic electron distribution on auroral emissions, *Trans. AGU, 68*, 1392, 1987*b*.

Lummerzheim, D., M. H. Rees, and H. R. Anderson, Angular dependent transport of auroral electrons in the upper atmosphere, in press, *Planet. Space Sci.*, 1989.

Phelps, A. D., and R. Sagalyn, Plasma density irregularities in the high-latitude topside ionosphere, *J. Geophys. Res., 81*, 515, 1976.

Rasmussen, C. E., R. W. Schunk, and V. B. Wickwar, A photochemical equilibrium model for ionospheric conductivity, *J. Geophys. Res., 93*, 9831, 1988.

Rees, M. H., Auroral ionization and excitation by incident energetic electrons, *Planet. Space Sci., 11*, 1209, 1963.

Rees, M. H., A. I. Stewart, W. E. Sharp, P. B. Hays, R. A. Hoffman, L. H. Brace, J. P. Doering, and W. K. Peterson, Coordinated rocket and satellite measurements of an auroral event, *J. Geophys. Res., 82*, 2250, 1977.

Rino, C. L., and S. J. Matthews, On the morphology of auroral zone radiowave scintillation, *J. Geophys. Res., 85*, 4139, 1979.

Robinson, R. M., R. T. Tsunoda, and J. F. Vickrey, Sources of *F* region ionization enhancements in the nighttime auroral zone, *J. Geophys. Res., 90*, 7533, 1985.

Roble, R. G., B. A. Emery, R. E. Dickinson, E. C. Ridley, T. L. Killeen, P. B. Hays, and G. R. Carignan, Theromspheric circulation, temperature, and compositional structure of the southern hemisphere polar cap during October–November 1981, *J. Geophys. Res., 98*, 9057, 1984.

Rodriguez, P., and E. P. Szuszczewicz, High-latitude irregularities in the lower *F* region: intensity and scale size distributions, *J. Geophys. Res., 89*, 5575, 1984.

Sato, T., and G. F. Rourke, *F* region enhancements in the Antarctic, *J. Geophys. Res., 69*, 4591, 1964.

Schunk, R. W., P. M. Banks, and W. J. Raitt, Effects of electric fields and other processes upon the nighttime high-latitude *F* layer, *J. Geophys. Res., 81*, 3271, 1976.

Sears, R. D., and R. R. Vondrak, Optical emissions and ionization profiles during an intense pulsating aurora, *J. Geophys. Res., 86*, 6853, 1981.

Sojka, J. J., and R. W. Schunk, A theoretical study of the production and decay of localized electron density enhancements in the polar ionosphere, *J. Geophys. Res., 91*, 3245, 1986.

Stamnes, K., W. J. Wiscombe, S. C. Tsay, and K. Jayaweera, An improved, numerically stable multiple scattering algorithm for discrete-ordinate-method radiative transfer in scattering and emitting layered media, *Appl. Opt., 27*, 2502, 1988.

Swartz, W. E., An optimization of energetic electron energy degradation calculations, *J. Geophys. Res., 90*, 6587, 1985.

Tsunoda, R. T., I. Häggström, A. Pellinen-Wannberg, Å. Steen, and G. Wannberg, Direct evidence of plasma density structuring in the auroral *F* region ionosphere, *Radio Sci., 20*, 762, 1985.

Vallance-Jones, A., R. L. Gattinger, P. Shih, J. Meriwether, V. B. Wickwar, and J. Kelly, Optical and radar characterization of a short-lived auroral event at high latitude, *J. Geophys. Res., 92*, 4575, 1987.

Vickrey, J. F., C. L. Rino, and T. A. Potemra, Chatanika/TRIAD observations of unstable ionization enhancements in the auroral *F* region, *Geophys. Res. Lett., 7*, 789, 1980.

Vondrak, R. R., and R. Robinson, Inference of high-latitude ionization and condctivity from AE-C measurements of auroral electron fluxes, *J. Geophys. Res., 90*, 7505, 1985.

Vondrak, R. R., and R. D. Sears, Comparison of incoherent scatter radar and photometric measurements of the energy distribution of auroral electrons, *J. Geophys. Res., 83*, 1665, 1978.

Weber, E., J. Buchau, J. G. Moore, J. R. Sharber, R. C. Livingston, J. D. Winningham, and B. W. Reinisch, *F* layer ionization patches in the polar cap, *J. Geophys. Res., 89*, 1683, 1984.

Weber, E. J., R. T. Tsunoda, J. Buchau, R. E. Sheehan, D. J. Strickland, W. Whiting, and J. G. Moore, Coordinated measurements of auroral zone plasma enhancements, *J. Geophys. Res., 90*, 6497, 1985.

Wickwar, V. B., M. J. Baron, and R. D. Sears, Auroral energy input from energetic electrons and Joule heating at Chatanika, *J. Geophys. Res., 80*, 4364, 1975.

K. D. Baker and J. LaBelle, Center for Atmospheric and Space Sciences, Utah State University, Logan, UT 84322.

G. Berg, G. D. Earle and M. C. Kelley, School of Electrical Engineering, Cornell University, Ithaca, NY 14853.

C. Kletzing, Department of Physics, University of California, San Diego, CA 92037.

D. Lummerzheim, Geophysical Institute, University of Alaska, Fairbanks, AK 99775.

R. J. Sica, Department of Physics, University of Western Ontario, London, Ontario, NGA 3K7.

R. B. Torbert, Department of Physics, University of Alabama, Huntsville, AL 35807.

(Received July 19, 1988;
revised November 3, 1988;
accepted November 4, 1988.)